A Theoretical Investigation of *p*-Hydroxyphenacyl Caged Phototrigger Compounds: An Examination of the Excited State Photochemistry of *p*-Hydroxyphenacyl Acetate

Xuebo Chen, Chensheng Ma, Wai Ming Kwok, Xiangguo Guan, Yong Du, and David Lee Phillips*

Department of Chemistry, The University of Hong Kong, Pokfulam Road, Hong Kong S.A.R., P. R. China

Received: July 15, 2006; In Final Form: September 18, 2006

Ab initio and density functional theory methods were employed to study the excited states and potential energy surfaces of the *p*-hydoxyphenacyl acetate (HPA) phototrigger compound. Complete active space (CAS) ab initio calculations predicted adiabatic electronic transition energies for the HPA-$T_1(^3n\pi^*)$, HPA-$T_2(^3\pi\pi^*)$, HPA-$S_1(^1n\pi^*)$, HPA-$T_3(^3n\pi^*)$, HPA-$S_2(^1n\pi^*)$, HPA-$S_3(^1\pi\pi^*) \leftarrow$ HPA-S_0 transitions that were similar to and in agreement with those found experimentally for closely related aromatic ketones such as *p*-hydroxyacetophenone and results from similar calculations for other related aromatic carbonyl systems. The α or β bond cleavage reactions from the S_1 excited state were both found to have relatively high barriers to reaction, and the S_1, T_1, and T_2 states are close in energy with the three $S_1(^1n\pi^*)$, $T_1(^3n\pi^*)$, and $T_2(^3\pi\pi^*)$ surfaces intersecting at the same region. The calculations suggest that intersystem crossing (ISC) can occur very fast from the S_1 state to the nearby triplet states. This is consistent with results from ultrafast spectroscopy experiments that observe the S_1 state ISC occurs within about 1−2 ps to produce a triplet state for HPA and related *p*HP compounds. The α and β bond cleavage reactions for the T_1 state of HPA are both predicted to have fairly high barriers and compete with one another. However, this is not completely consistent with experiments that observe the photodeprotection reactions (e.g. the β bond cleavage) of HPA and some other *p*HP phototriggers in largely water containing solvents are predominant and occur very fast to release the leaving group. Comparison of the computational results with experimental results for HPA and related *p*HP compounds suggests that water molecules likely play an important part in changing the triplet state β bond cleavage so that it becomes the predominant pathway and occurs very fast to give an efficient deprotection reaction. The results reported here provide new insight into the photophysics, reaction pathways, and photochemistry of the *p*-hydoxyphenacyl acetate and related *p*HP caged phototrigger compounds and also provide a benchmark for further and more sophisticated investigations in the future.

Introduction

There is much interest among a wide range of scientists in cage compounds and their applications in synthesis and as phototriggers in biological experiments.[1,2] There is increasing attention being given to developing efficient cage compounds for use as phototriggers that can be employed for real-time monitoring of physiological responses in biological systems.[1−8] The *p*-hydroxyphenacyl (*p*HP) protecting group has been of particular interest because of its practical potential as a rapid and efficient "cage" for the release of a variety of biological stimulants.[9−11] The products and reaction conditions for *p*HP deprotection have been extensively studied and are fairly well-known.[12−14] However, the reaction mechanism(s) for the photodeprotection reaction s of *p*HP caged compounds is not well understood. In particular, there is still some uncertainty about the events and reactive intermediates involved in the photochemical pathway.

A number of experimental studies have been done to characterize the intermediates and pathways involved in the photodeprotection and photosolvolytic reactions of *p*HP caged compounds. Givens, Wirz, and co-workers[12] and Wan and co-workers[13] employed time-resolved transient absorption (TA) spectroscopy to observe several short-lived intermediates after ultraviolet (~300 nm) excitation of *p*HP caged acetate (HPA) and diethyl phosphate (HPDP) in aqueous containing solvents. However, these studies did not provide an unambiguous interpretation of the data, and several different reaction mechanisms have been proposed to account for the photodeprotection and photosolvolytic reactions.[12,13] We have done further studies employing a combination of femtosecond Kerr gated time-resolved fluorescence (KTRF) and picosecond time-resolved resonance Raman (TR^3) spectroscopy[15] on the HPA and HPDP systems, and this work gave explicit evidence that the triplet state is the reactive precursor for the *p*HP photodeprotection reaction. We have also recently used sub-picosecond TA and ps-TR^3 to investigate the HPDP and newly synthesized *p*HP caged diphenyl phosphate (HPPP) phototriggers in H_2O/MeCN mixed solvent systems.[16] TA spectroscopy was employed to examine the solvent decay dynamics of the triplet state precursor to deprotection, and TR^3 spectroscopy was utilized to follow the formation dynamics of the HPA rearrangement product in the mixed solvent systems.[16] An overall reaction mechanism was proposed based on these experimental results for the deprotection and rearrangement reactions for the pHP caged phosphate compounds.[16]

While the photodeprotection reactions of *p*HP cage compounds have been extensively studied by experimental methods

* Author to whom correspondence should be addressed. Tel: 852-2859-2160. Fax: 852-2957-1586. E-mail: phillips@hkucc.hku.hk.

10.1021/jp064490e CCC: $33.50
Published on Web 10/25/2006

over the past decade, there has been little theoretical work done to better understand the photophysics and photochemistry of these important reactions. Here, we present a theoretical investigation of the excited states and potential energy surfaces of the *p*-hydoxyphenacyl acetate phototrigger compound. The results presented here provide new insight into the photophysics, reaction pathways, and photochemistry of the *p*-hydoxyphenacyl acetate compound and related *p*HP caged phototrigger compounds. Our preliminary study reported here for the excited states of the *p*-hydoxyphenacyl acetate compound also provides a benchmark for further and more sophisticated investigations of the intriguing and important photochemistry of *p*HP caged phototrigger compounds.

Computational Methods

Stationary structures for the *p*-hydroxyphenacyl acetate (HPA) molecule in its seven lowest electronic states (S_0, S_1, S_2, S_3, T_1, T_2, and T_3) have been fully optimized by employing the complete active space self-consistent field (CASSCF) method. The B3LYP density functional theory method was also utilized to determine the geometric structures for HPA, HPDP, and HPPP in their ground and triplet states. In this work, the 6-31G* and 6-31G basis sets were chosen and used in the CASSCF and B3LYP calculations. All of the computations reported here were carried out using the Gaussian 03 suite of quantum chemical programs.[17] After preliminary CASSCF calculations using the CAS(10,8)/6-31G level of theory, all of the stationary structures were reoptimized at the CAS(14,11)/6-31G* level of theory. For the computed equilibrium geometries on the S_0, S_1, S_3, T_1, and T_2 surfaces, 14 electrons and 11 orbitals were used in the calculations. These electrons and orbitals originate from the carbonyl C8═O11 and C12═O13 (see the numbering scheme in Figures 1) π orbitals and C8═O11 π^* orbital, the *p*-hydroxy O7 and O11 nonbonding orbitals, and three π and three π^* orbitals in the aromatic ring. When this (14, 11) active space was employed to optimize the structures in the T_3 and the S_2 surfaces, the C8═O11 π^* and O11 nonbonding orbitals were replaced by the C12═O13 antibonding and O13 nonbonding orbitals. Structural optimizations of the surface intersections were performed with the two root state-averaged CASSCF method. Since the state-averaged calculations are very time-consuming and due to the limitations of the available computer memory in our laboratory, the (10, 8) active space was used to search for the lowest energy point of the surface crossing seam. To investigate solvent effects on the α and β bond fissions of HPA in the triplet states, we reoptimized the stationary structures along the two reactive channels using self-consistent reaction field (SCRF) methods at the B3LYP level of theory. The polarizable continuum model (PCM) was introduced in the present calculations, and the dielectric constants were set to 78.39, 36.64, and 2.247 for water, acetonitrile, and benzene, respectively. In this work, all of the stationary structures were confirmed to be minima or first-order saddle points by analytical frequency calculations at the B3LYP/6-31G* and CAS(10,8)/6-31G levels of theory. The zero point energy corrections were applied to the relative energies without using any scaling factor.

Results and Discussion

A. The C9−C8 and C9−O10 Bond Cleavage Pathways in the Ground and Excited Triplet and Singlet States of HPA. *1. The Equilibrium Structures of the S_0, S_1, S_2, S_3, T_1, T_2, and T_3 States.* The equilibrium structures for HPA in its lowest seven electronic states (HPA-S_0, HPA-S_1, HPA-S_2, HPA-S_3, HPA-T_1, HPA-T_2, and HPA-T_3) were optimized and confirmed to be minima by CASSCF calculations. These structures are schematically listed in Figure 1 with a numbering scheme shown for the HPA-S_0 structure. The computed relative energies for these states are summarized in Table 1. The planar and nonplanar minimum structures for HPA-S_0 were also found by B3LYP/6-31G* optimization, which was further reproduced by CAS(14,11)/6-31G* calculations. As shown in Figure 1, the −O10C12O13C14H_3 (−OAc) group in HPA-S_0 appears with a torsional rotation out of the plane by 60.9° at the CAS(14,-11)/6-31G* level of theory. The planar minimum of the HPA-S_0 is located 1.07 kcal/mol above the nonplanar HPA structure in the ground state at the CAS(14,11)/6-31G* level of theory. Meanwhile, the energy gaps between the planar (quasi-planar) and twisted minimum structures for HPA in the T_2, T_3, S_2, and S_3 states were also computed to be 1.60, 2.20, 1.32, and 1.02 kcal/mol, respectively, at the CAS(14,11)/6-31G* level of theory. This energetic proximity between the two isomers indicates that the planar and twisted minima of HPA are coexistent in the lowest several electronic states. In this work, we employed the twisted minimum structures of HPA to serve as reactants in elucidating mechanistic pathways for the photodeprotection in the primary photochemical step.

With respect to the HPA-S_0 structure, the most striking changes in the HPA-T_1 or HPA-S_1 structures occur in the C8−O11 bond length. As illustrated in Figure 1, the C8−O11 bond length is 1.210 Å in HPA-S_0, while it is elongated to become 1.351 Å in HPA-T_1 and 1.363 Å in HPA-S_1, respectively. A molecular orbital analysis shows that the two singly occupied electrons are distributed in the C8═O11 π^* orbital and the O11 nonbonding orbital, respectively, which indicates that HPA-T_1 and HPA-S_1 originate from a $n\rightarrow\pi^*$ transition. Similarly, the $n\rightarrow\pi^*$ transition of the C12═O13 carbonyl lead to a pyramidal −O10C12O13C14H_3 (−OAc) group in the structures of HPA-T_3 and HPA-S_2. The C12−O13 bond is significantly increased by 0.180 and 0.195 Å from HPA-S_0 to HPA-T_3 and HPA-S_2, which is accompanied by a decrease of the dihedral O10C12O-13C14 angle from 180° in HPA-S_0 to ∼130° in HPA-T_3 and HPA-S_2. Meanwhile, the conjugation between the O10 2p orbital and the C12═O13 π orbital has been weakened, causing the C12−O10 bond length to become elongated to ∼1.354 Å in HPA-T_3 and HPA-S_2, while it is 1.331 Å in the ground state.

As mentioned above, there are similar minimum structures between the $n\rightarrow\pi^*$ excited singlet (HPA-S_2 and HPA-S_1) and triplet (HPA-T_1 and HPA-T_3) states. However, the main structural differences were found between the $^3\pi\pi^*$ and $^1\pi\pi^*$ minima. The C1−C2 and C4−C5 bond lengths in HPA-T_2 are 1.358 and 1.360 Å, respectively, which appear to have double bond character. However, other C−C bonds in the aromatic ring exhibit single bond character and the C2−C3, C3−C4, C6−C1, and C6−C5 bond lengths were determined to be 1.444, 1.440, 1.481, and 1.484 Å, respectively, by CAS(14,11)/6-31G* calculations. The structure of HPA-T_2 is a diradical where the two singly occupied electrons are distributed on the C3 and C6 atom region, respectively, which is confirmed by a molecular orbital analysis. Like HPA-T_2($^3\pi\pi^*$), the $\pi\rightarrow\pi^*$ singlet transition for HPA is also mainly localized on the aromatic ring. The two unpaired electrons are delocalized to the whole phenyl ring, which is responsible for the structural formation of an "enlarged" benzene ring in HPA-S_3. The C−C bond lengths in the aromatic ring are nearly equal and range between 1.42 and 1.44 Å in HPA-S_3($^1\pi\pi^*$), while they are ∼1.40 Å in the ground state.

It has long been recognized that the importance of energetic proximity between nπ^* and $\pi\pi^*$ triplet states for aromatic ketones (PhC(═O)R) is susceptible to substituent effects and

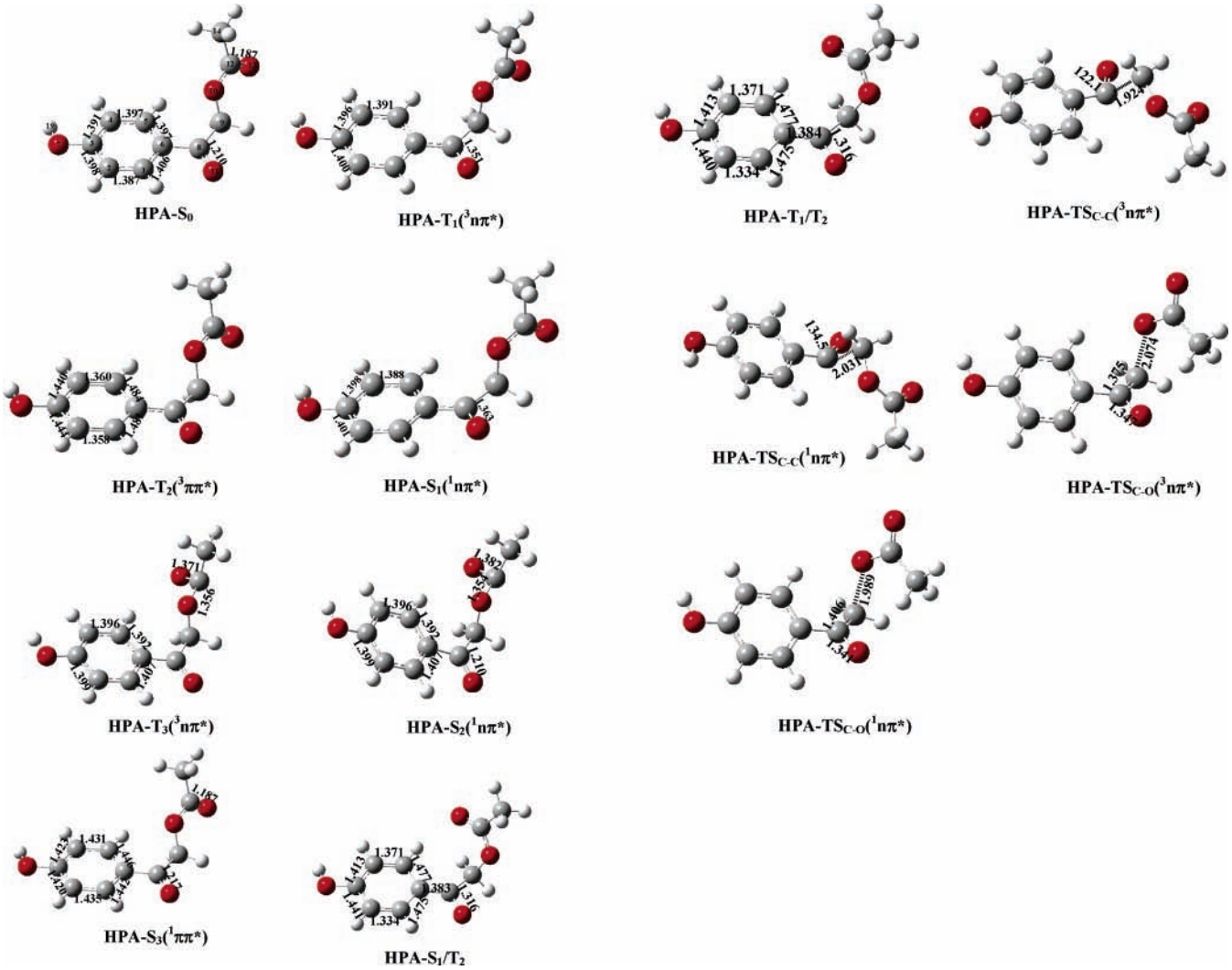

Figure 1. Schematic structures of stationary and intersection points for *p*-hydroxyphenacyl acetate (HPA) along with the selected bond lengths (Å) and the atom labeling scheme in the S_0 structures.

TABLE 1: The Relative Energies (in kcal/mol) for *p*-Hydroxyphenacyl Acetate (HPA) in the Lowest Seven States at the CAS(14,11)/6-31G* Level[a]

HPA-S_0	0.0	HPA-$T_3(^3n\pi^*)$	92.7 (91.2)
HPA-$T_1(^3n\pi^*)$	73.5 (71.5)	HPA-$S_2(^1n\pi^*)$	98.4 (97.0)
HPA-$S_1(^1n\pi^*)$	77.3 (75.0)	HPA-$S_3(^1\pi\pi^*)$	107.3 (103.4)
HPA-$T_2(^3\pi\pi^*)$	76.1 (72.9)		

[a] The values in parentheses with the CAS(10,8)/6-31G zero point energy correction.

solvent polarity.[18,19] Unsubstituted phenyl ketones have a $n\pi^*$ lowest triplet state with a $\pi\pi^*$ triplet state a few kcal/mol higher in energy.[18d,20] The electron-donation substituent in benzene ring lowers the $\pi\pi^*$[18b,21] and promotes the $n\pi^*$ transition energies.[22−24] This close energy spacing between the $n\pi^*$ and $\pi\pi^*$ triplet states for aromatic ketones was well reproduced by our previous CASSCF calculations in a series of examples of phenyl carbonyl compounds.[25−27] Moreover, our calculations predict that the electron-donation substituent in the C atom of the carbonyl group for aromatic ketones causes an inversion of the triplets with a large energy gap, where the $\pi\pi^*$ state is ~12.0 kcal/mol lower than the $n\pi^*$ state in energy.[28] As far as we know, there have been no reports on the detailed electronic spectroscopic properties of HPA (p-$OHC_6H_4COCH_2-OCOCH_3$). However, these spectroscopic properties for analogous aromatic ketones have been experimentally well established. The band origins to $^3n\pi^*$, $^3\pi\pi^*$, $^1n\pi^*$, and $^1\pi\pi^*$ have been observed to be 72.0 (25 183 cm^{-1}),[29] 76.1 (3.3 eV),[30] 76.9 (26 919 cm^{-1}),[29] and 100.6 kcal/mol (35191 cm^{-1})[31] for PhCHO and 73.7 (25 791 cm^{-1}),[30] 77.9 (27 279 cm^{-1}),[29] and 101.2 kcal/mol (35 402 cm^{-1})[32] to the $^3n\pi^*$, $^1n\pi^*$, and $^1\pi\pi^*$ states of $PhC(=O)CH_3$.

As shown in Table 1, adiabatically, the HPA-$T_1(^3n\pi^*)$, HPA-$T_2(^3\pi\pi^*)$, HPA-$S_1(^1n\pi^*)$, HPA-$T_3(^3n\pi^*)$, HPA-$S_2(^1n\pi^*)$, HPA-$S_3(^1\pi\pi^*)$ ← HPA-S_0 transitions were determined to be 71.5, 72.9, 75.0, 91.2, 97.0, and 103.4 kcal/mol by the CAS(14,11)/6-31G* calculations with a CAS(10,8)/6-31G zero point energy correction. In our present calculations, the energy gap between the $\pi\pi^*$ and $n\pi^*$ triplet states is 1.4 kcal/mol, which is narrower than that of PhCHO, which has a value of 4.1 kcal/mol.[29,30] In agreement with previous experimental observations,[18b, 21] the para substituent with an electron-donating hydroxyl group on the benzene ring of HPA slightly influences the energy levels of the $^3n\pi^*$ and $^3\pi\pi^*$ states, where the two triplet states come closer in energy. The HPA-$T_2(^3\pi\pi^*)$ (72.9 kcal/mol) lies sandwiched between the HPA-$T_1(^3n\pi^*)$ (71.5 kcal/mol) and HPA-$S_1(^1n\pi^*)$ (75.0 kcal/mol) in energy, which is consistent with Kearns's energy levels ordering for a number of aromatic ketones using the phosphorescence excitation method.[21d,e] In Kearns's experimental investigation, the $S_1(^1n\pi^*)$ absorption is found to be at ~346 nm (vertical excitation energy 82.6 kcal/mol) for *p*-hydroxyacetophenone. In comparison with the

corresponding experimental values, the present computations give a reasonable estimate for the relative energies of the low-lying electronic states of *p*-hydroxyphenacyl acetate. As explained in our previous calculations for a series of aromatic carbonyl compounds,[25−28] the π and σ orbitals are energetically well-separated in HPA with large π conjugation systems, and the near-degenerate orbitals could be chosen in the CAS(14,-11) active space, which is responsible for the accurate predictions of the adiabatic energies for HPA.

2. $S_1(^1n\pi^*)$, $T_1(^3n\pi^*)$, and $T_2(^3\pi\pi^*)$ Three Surface Intersection for HPA. Since there is a close energy spacing between the $n\pi^*$ and $\pi\pi^*$ triplet states of HPA, it is reasonable to expect that these two lowest triplet surfaces intersect at some point. The two triplet state surface crossing for HPA has been optimized using a state-averaged CAS(10,8)/6-31G* approach and assigned to be a conical intersection between the $T_1(^3n\pi^*)$ and $T_2(^3\pi\pi^*)$ surfaces based on the structural characteristics and the relative energies with respect to the corresponding minima as well as the one electron density matrix. The intersection between the $S_1(^1n\pi^*)$ and $T_2(^3\pi\pi^*)$ surfaces, meanwhile, was also determined by using the Slater determinants in the SA-CAS(10,8)/6-31G* calculations. Comparison of the HPA-T_1/T_2 and HPA-S_1/T_2 intersections found that they were essentially indistinguishable in structure and energy, and this indicates that the three $S_1(^1n\pi^*)$, $T_1(^3n\pi^*)$ and $T_2(^3\pi\pi^*)$ surfaces intersect at the same region. An analogous three surface intersection was also found in a series of unsubstituted phenyl ketones (PhC(═O)R).[25−28] The benzene ring in HPA-T_1/T_2 (HPA-S_1/T_2) exhibits a structural characteristic of "four longer and two shorter" where the C1−C2 and C4−C5 bond lengths in HPA-T_1/T_2 are 1.334 and 1.371 Å, respectively, with double bond character while the other C−C bonds in the aromatic ring have single bond character with their lengths in the 1.41−1.47 Å range. Structurally, the benzene ring moiety of HPA-T_1/T_2 (HPA-S_1/T_2) is similar to the HPA-$T_2(^3\pi\pi^*)$ minimum with a 1,4-diradical configuration. At the same time, the bond parameters in the carbonyl C8−O10 moiety of HPA-T_1/T_2 (HPA-S_1/T_2) are observed to be very close to that of the HPA-$S_1(^1n\pi^*)$ or HPA-$T_1(^3n\pi^*)$ minimum, where the carbonyl C8−O10 is elongated to become 1.316 Å. Meanwhile, a π bond is formed between single electrons that are distributed on the C6 and C8 atoms, which leads to the double bond character of C6═C8 (1.383 Å). Obviously, HPA-T_1/T_2 (or HPA-S_1/T_2) is well equilibrated with excitation between the two chromophores of the aromatic ring and the carbonyl moieties. The HPA-T_1/T_2 (HPA-S_1/T_2) with single electrons located on the C6 and C11 region lies about midway between an electronic redistribution from the HPA-$S_1(^1n\pi^*)$ (or HPA-$T_1(^3n\pi^*)$) to HPA-$T_2(^3\pi\pi^*)$ to minimum. The HPA-T_1/T_2 (HPA-S_1/T_2) is 3.89 kcal/mol above the HPA-$S_1(^1n\pi^*)$ minimum in energy at the CAS(10,8)/6-31G* level of theory.

3. The C8−C9 and C9−O10 Bond Dissociation on the Ground State Surfaces. The dissociation of *p*-hydroxyphenacyl acetate (*p*-$OHC_6H_4COCH_2-OCOCH_3$) along the two C8−C9 and C9−O10 bond fission reactions in the ground state could lead to the corresponding radical pairs: *p*-$OHC_6H_4CO(\tilde{X},^2A')$ + $CH_2OCOCH_3(\tilde{X},^2A)$ and *p*-$OHC_6H_4COCH_2(\tilde{X},^2A')$ + $OCOCH_3(\tilde{X},^2A')$, respectively. The attempts for optimization of the transition states along the C8−C9 and C9−O10 bond cleavage pathways in the ground state at CAS(14,11)/6-31G* and B3LYP/6-31G* levels always converged to the dissociation limit of *p*-OHC_6H_4CO + $CH_2-OCOCH_3$ and *p*-$OHC_6H_4COCH_2$ + $OCOCH_3$ instead of the first-order saddle points for bond fission in the ground state. These results suggest that there exists no potential barrier above endothermicity on the S_0 pathway. The endothermic energies were determined to be 79.8 and 56.1 kcal/mol for C8−C9 and C9−O10 bond fission by supermolecule optimizations at the CAS(14,11)/6-31G* level of theory with a CAS(10,8)/6-31G zero point energy correction included. At the B3LYP/6-31G* level of theory with a zero point energy correction, the endothermic energies of HPA, HPDP, and HPPP were calculated to be 77.3, 70.3, and 72.8 kcal/mol for the C8−C9 bond and 67.1, 65.9, and 63.5 kcal/mol for the C9−O10 bond (see the Supporting Information). These results indicate that the β fission (C9−O10 bond) of the *p*-hydroxyphenacyl caged phototrigger compounds is easier than the α scission (C8−C9 bond) in the ground state.

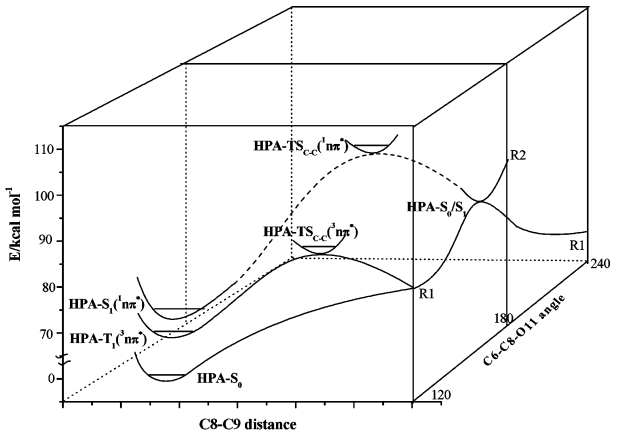

$$R1 = p-OHC_6H_4\dot{C}O(\tilde{X},^2A') + \dot{C}H_2OCOCH_3(\tilde{X},^2A)$$

$$R2 = p-OHC_6H_4\dot{C}O(\tilde{A},^2A'') + \dot{C}H_2OCOCH_3(\tilde{X},^2A)$$

(a)

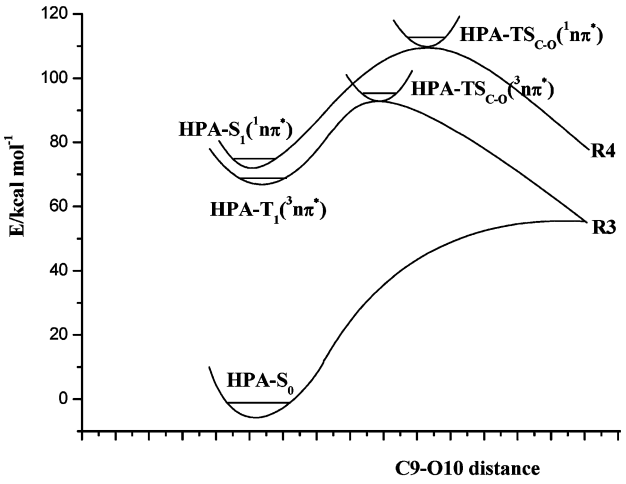

$$R3 = p-OHC_6H_4CO\dot{C}H_2\ (\tilde{X},^2A') + \dot{O}COCH_3\ (\tilde{X},^2A')$$

$$R4 = p-OHC_6H_4C\dot{O}CH_2\ (\tilde{X},^2A) + \dot{O}COCH_3\ (\tilde{X},^2A')$$

(b)

Figure 2. Schematic potential energy surface of α (a) and β (b) bond fissions for *p*-hydroxyphenacyl acetate (HPA) in the ground, $^3n\pi^*$, and $^1n\pi^*$ states along with relative energies (kcal/mol) at the CAS(14,11)/6-31G* level of theory with CAS(10,8)/6-31G zero point correction.

4. C8−C9 and C9−O10 Bond Fission in the $^3n\pi^*$ State Surfaces. As shown in potential energy profiles for C8−C9 bond fission (see Figure 2a), the transition state of HPA-$TS_{C-C}(^3n\pi^*)$ connects the corresponding reactant and product in the triplet

reaction pathway. The structure of HPA-$TS_{C-C}(^3n\pi^*)$ was optimized and listed in Figure 1 at the CAS(14,11)/6-31G* level of theory. The distance between C9 and C8 is 1.924 Å in HPA-$TS_{C-C}(^3n\pi^*)$, while it is 1.492 Å in the HPA-$T_1(^3n\pi^*)$ minimum at the CAS(14,11)/6-31G* level of theory. The reoptimizations of HPA-$T_1(^3n\pi^*)$ using B3LYP/6-31G* calculations show that the C9−C8 bond is increased by 0.565 Å from 1.502 Å in HPA-$T_1(^3n\pi^*)$ to 2.067 Å in HPA-$TS_{C-C}(^3n\pi^*)$. To ascertain the nature of state involving the C8−C9 bond fission, the IRC calculations were carried out at both CASSCF and B3LYP levels of theory. In the direction of the product, the transition state was found to connect the ground state radical pair *p*-$OHC_6H_4CO(\tilde{X},^2A')$ + $CH_2OCOCH_3(\tilde{X},^2A)$. Toward the other side, with a decreasing of the C8 and C9 distance, the C8−O11 bond length was gradually elongated in the IRC pathway toward the reactant. Finally, the geometric structures of the IRC calculations are close to those of the HPA-$T_1(^3n\pi^*)$ minima at the CASSCF and B3LYP levels of theory. These findings suggest that the transition state of HPA-$TS_{C-C}(^3n\pi^*)$ connects with the HPA-$T_1(^3n\pi^*)$ minimum, which implies that a C9−C8 bond scission takes place in the lowest $n\pi^*$ triplet state. The barrier of the C8−C9 bond scission in the $T_1(^3n\pi^*)$ state is predicted to be 11.2 kcal/mol at the CAS(14,11)/6-31G* level of theory with a CAS(10,8)/6-31G zero point energy correction. Similar transition state structures were found for the $n\pi^*$ triplet state C8−C9 bond fission of HPDP and HPPP at the B3LYP/6-31G* level of theory (see the Supporting Information). The barriers of T_1 C8−C9 bond scission for HPA, HPDP, and HPPP were determined to be 15.9, 14.9, and 16.6 kcal/mol, respectively, at the B3LYP/6-31G* level of theory with a zero point energy correction. This implies that different leaving groups only slightly influence the barrier of C8−C9 bond cleavage in the $T_1(^3n\pi^*)$ state.

Similarly, β bond fission (C9−O10 bond) of HPA in the triplet state emanates from the HPA-$T_1(^3n\pi^*)$ minimum (see Figure 2b). However, the structure of HPA-$TS_{C-O}(^3n\pi^*)$ differs from that of HPA-$TS_{C-C}(^3n\pi^*)$. As illustrated in Figure 1, the C8−O11 bond length is 1.347 Å in HPA-$TS_{C-O}(^3n\pi^*)$, which is longer than that in HPA-$TS_{C-C}(^3n\pi^*)$ (1.258 Å) and similar to the HPA-$T_1(^3n\pi^*)$ minimum (1.351 Å). Normally, the C−O bond is significantly shortened with respect to the corresponding minimum in the α bond scission of carbonyl compounds induced by a $n\rightarrow\pi^*$ transition.[33−37] In the β bond fission of HPA, however, the C−O bond remains unchanged from the HPA-$T_1(^3n\pi^*)$ minimum to HPA-$TS_{C-O}(^3n\pi^*)$, which implies that the $n\rightarrow\pi^*$ excitation causes little influence on the β bond fission due to the distribution of excited energies in the region of the α bond. The barrier of the β bond fission (C9−C10) for HPA, HPDP, and HPPP was predicted to be 17.4, 12.2, 7.1 kcal/mol, respectively, at the B3LYP/6-31G* level of theory with a zero point energy correction included, whereas, at the CAS(14,11)/6-31G* level of theory with a CAS(10,8)/6-31G zero point energy correction, the cleavage of C9−O10 for HPA must overcome a 20.7 kcal/mol barrier. Comparing the barriers of β bond fission with those of α bond fission for the three molecules in the $T_1(^3n\pi^*)$ state, we can draw a conclusion that the α bond fission is easier than β bond fission upon excitation of the $n\rightarrow\pi^*$ transition and the two cleavage channels may compete with each other in the $T_1(^3n\pi^*)$ state. A series of photochemical investigations of related phenacyl sulfides $PhC(=O)CH_2SR$, $PhC(=O)CH_2S(O)R$, $PhC(=O)CH_2SO_2R$, and *p*-X-PhC(=O)CHSPh revealed that the β-cleavage competed with other triplet state reactions and the maximum quantum yield for this β-cleavage was 0.40.[38] Obviously, the favorable cleavage channel is inversed between the ground and the $T_1(^3n\pi^*)$ states. The distribution of the excited energies in the region of the α bond could weaken the C8−C9 bond and does not influence the intensity of the C9−O10 bond, which accounts for the inversion of the favorable cleavage channel upon excitation of the $n\rightarrow\pi^*$ transition.

5. C8−C9 and C9−O10 Bond Scission in the $^1n\pi^*$ State Surfaces. As mentioned above, the radical pair *p*-$OHC_6H_4CO(\tilde{X},^2A')$ + $CH_2OCOCH_3(\tilde{X},^2A)$ correlates with HPA-S_0 and HPA-$T_1(^3n\pi^*)$, respectively. Qualitatively, the C8−C9 fission for HPA in the excited singlet state can decay to radical fragments in the excited state. As illustrated in the potential energy profile of the C9−C8 fission (see Figure 2a), the two main reaction coordinates of the C9−C8 distance and the C6C8O9 angle correspond to $S_1(^1n\pi^*)$ C9−C8 scission, while only one main reaction coordinate of the C8−C9 distance is involved in the $T_1(^3n\pi^*)$ dissociation pathway. The transition state HPA-$TS_{C-C}(^1n\pi^*)$ in the excited singlet state was found and confirmed to be the first saddle point by CASSCF calculations. The barrier was determined to be 35.7 kcal/mol by CAS(14,11)/6-31G* calculations with a CAS(10,8)/6-31G zero point energy correction. The C8−C9 distance was calculated to be 2.031 Å in HPA-$TS_{C-C}(^1n\pi^*)$ at the CAS(14,11)/6-31G* level of theory and 0.107 Å longer than that in HPA-$TS_{C-C}(^3n\pi^*)$. The other structural differences between HPA-$TS_{C-C}(^1n\pi^*)$ and HPA-$TS_{C-C}(^3n\pi^*)$ are associated with the C6C8O11 angle. As illustrated in Figure 1, the C6C8O11 angle is increased to 134.5° in HPA-$TS_{C-C}(^1n\pi^*)$, while it is 122.1° in HPA-$TS_{C-C}(^3n\pi^*)$. The structural differences between the two transition states provide clues that the two transition states connect products in different electronic states. The IRC calculations starting from HPA-$TS_{C-C}(^1n\pi^*)$ confirmed a connection with the $S_1(^1n\pi^*)$ minimum on the IRC pathway towards the reactant. On the other side, however, the problem of convergence was encountered during the state-specific CASSCF calculations of the IRC pathway with the C9−C8 separation found at 2.56 Å. Energetically, the S_0 and S_1 states come closer to each other when the separation of the *p*-OHC_6H_4CO and CH_2OCOCH_3 radicals is far enough. The state-averaged CAS(10,8)/6-31G optimizations found a conical intersection between the S_0 and S_1 surfaces (HPA-S_0/S_1) at a C8 and C9 separation of 2.778 Å. Besides the increased C9−C8 distance, the most striking structural change is associated with an increase of the C6C8O11 angle from 118.8° in HPA-$S_1(^1n\pi^*)$ to 134.5° in HPA-$TS_{C-C}(^1n\pi^*)$ and to 166.4° in HPA-S_0/S_1.

To elucidate the nature of the electronic state for the dissociation products, the structure of the *p*-OHC_6H_4CO radical in the ground and first excited states was optimized by CAS(9,8)/6-31G* calculations. The *p*-OHC_6H_4CO radical in the ground and first excited states adopts A′ and A″ symmetry, respectively, and their adiabatic energetic gap was determined to be 6.1 kcal/mol at the CAS(9,8)/6-31G* level of theory. The most striking structural change is associated with the C6C8O9 angle from *p*-$OHC_6H_4CO(\tilde{X},^2A')$ where it is 129.0° to *p*-$OHC_6H_4CO(\tilde{A},^2A'')$ where it is nearly 180.0° at the CAS(9,8)/6-31G* level of theory. The single electron locates in the molecular plane in *p*-$OHC_6H_4CO(\tilde{X},^2A')$, while it populates a perpendicular orientation to the molecular skeleton. From the viewpoint of valence theory, the C8 atom of *p*-OHC_6H_4CO rehybridizes from sp^2 in the ground state to sp in the first excited state, which is responsible for the structural changes caused by electron excitation. These findings explain why the C6C8O9 angle is gradually increased from the $S_1(^1n\pi^*)$ minimum to the transition state and then to the potential energy surface intersection along the $S_1(^1n\pi^*)$ state C9−C8 bond scission pathway. The intersec-

tion of HPA-S_0/S_1 is 2.2 kcal/mol lower HPA-$TS_{C-C}(^1n\pi^*)$ in energy at the CAS(10,8)/6-31G level of theory. The gradient difference and nonadiabatic coupling vectors of HPA-S_0/S_1 show that this conical intersection could decay to the *p*-$OHC_6H_4CO(\tilde{X},^2A')$ + $CH_2OCOCH_3(\tilde{X},^2A)$ fragments in the ground state. In summary, the S_1 state C9−C8 bond scission starting from the HPA-$S_1(^1n\pi^*)$ minimum overcomes a 35.7 kcal/mol HPA-$TS_{C-C}(^1n\pi^*)$ barrier, and finally funnels through HPA-S_0/S_1 down to the *p*-$OHC_6H_4CO(\tilde{X},^2A')$ + $CH_2OCOCH_3(\tilde{X},^2A)$ fragments in the ground state. Considering the relatively high barrier, $S_1(^1n\pi^*)$ α bond fission takes place with substantial difficulty.

Unlike the $S_1(^1n\pi^*)$ α bond cleavage, the mechanism for $S_1(^1n\pi^*)$ *β* bond fission for HPA seems "simpler" (see Figure 2b). A HPA-$TS_{C-O}(^1n\pi^*)$ transition state was found by CASSCF optimization along the $S_1(^1n\pi^*)$ C9−O10 bond fission pathway. IRC/CASSCF calculations confirmed that HPA-$TS_{C-O}(^1n\pi^*)$ connects with the HPA-$S_1(^1n\pi^*)$ minimum in the direction of reactant. On the other side, the C8−O11 bond was gradually elongated (longer than 1.380 Å) and the C8═C9 bond gradually exhibited double bond character (around 1.320 Å) in the direction of product. These results imply that the HPA-$TS_{C-O}(^1n\pi^*)$ connects with the *p*-$OHC_6H_4\dot{C}OCH_2(\tilde{X},^2A)$ radical in which a singly occupied electron distributes over the O11 region rather than *p*-$OHC_6H_4CO\dot{C}H_2(\tilde{X},^2A')$ in which the singly occupied electron locates on the C9 atom. The distance of C9−O10 in HPA-$TS_{C-O}(^1n\pi^*)$ increases to 1.989 Å from 1.425 Å in the HPA-$S_1(^1n\pi^*)$ minimum. The C8−O11 bond of HPA-$TS_{C-O}(^1n\pi^*)$ appears have a single bond character with a bond length of 1.341 Å, which indicates that the excited singlet *β* bond fission is induced by a n→p* transition. With respect to HPA-S_0 and HPA-$S_1(^1n\pi^*)$, the barriers of HPA-$TS_{C-O}(^1n\pi^*)$ are 110.5 and 35.5 kcal/mol at the CAS(14,11)/6-31G* level of theory, respectively. This indicates that the occurrence of $S_1(^1n\pi^*)$ *β* bond fission is not easy.

6. Solvent Effects on the α and β Bond Fissions of HPA on the nπ Triplet State Surfaces.* To ascertain the role of water in the photochemical processes of *p*-hydroxyphenacyl caged phototrigger compounds, we considered water as a solvent. For comparison, we also employed acetonitrile and benzene as solvents to elucidate solvent effects on the α and *β* bond fissions of HPA in the nπ* triplet state**.** The structures of the minimum of the ground state and the transition states for the α and *β* bond fissions of HPA on the nπ* triplet state were reoptimized in the solvent systems of water, acetonitrile, and benzene using SCRF/PCM methods at the B3LYP/6-31G* level of theory. The optimized structures (Cartesian coordinates) and energies obtained are listed in the Supporting Information.

The transition state of the α bond scission of HPA on the triplet state (HPA-$TS_{C-C}(^3n\pi^*)$) was obtained by SCRF/PCM//B3LYP/6-31G* calculations using a dielectric constant of 78.39 (for water). This transition state was confirmed by IRC calculations to be connected with the HPA-$T_1(^3n\pi^*)$ minimum and the radical pair *p*-$OHC_6H_4CO(\tilde{X},^2A')$ + $CH_2OCOCH_3(\tilde{X},^2A)$. The C8−C9 distance in HPA-$TS_{C-C}(^3n\pi^*)$ is 2.052 Å at the SCRF/PCM(water)//B3LYP/6-31G* level of theory, and this is similar to the 2.067 Å distance at the B3LYP/6-31G* level of theory. With respect to the HPA-S_0(water) zero level, the barrier of HPA-$TS_{C-C}(^3n\pi^*)$ is 81.8 kcal/mol at the SCRF/PCM(water)//B3LYP/6-31G* level of theory with the zero point correction included, which is consistent with the barrier (81.3 kcal/mol) of nπ* triplet state α bond cleavage in the gas phase. For the same calculations and zero level, the barrier of the *β* bond fission (HPA-$TS_{C-O}(^3n\pi^*)$) is 76.6 kcal/mol, which is lower than that in the gas phase (82.8 kcal/mol). Similarly, in the polar acetonitrile solvent, the barrier of the α bond cleavage on the nπ* triplet state was calculated to be 81.9 kcal/mol with respect to the HPA-S_0 (acetonitrile) zero level at the SCRF/PCM(acetonitrile)//B3LYP/6-31G* level of theory with the zero point energy correction included while the barrier of the *β* bond fission was determined to be 76.8 kcal/mol for the same calculations and zero levels. However, in the nonpolar benzene solvent, the barriers of the nπ* triplet state α and *β* bond cleavage reactions were determined to be 81.6 and 81.0 kcal/mol, respectively, with respect to the HPA-S_0 (benzene) zero level at the SCRF/PCM(benzene)//B3LYP/6-31G* level of theory with the zero point energy correction included, which is consistent with those in the gas phase for both the α (81.3 kcal/mol) and *β* (82.8 kcal/mol) bond fission channels. These calculations imply that a polar solvent causes the *β* bond fission to become the more favorable channel in comparison with a more competitive mechanism in the gas phase. However, the nonpolar solvent does not change the barrier along the two scission channels in the nπ* triplet state very much compared to the gas phase mechanism.

B. Discussion of Results. We note that the adiabatic electronic transition energies from the CAS(14,11)/6-31G* calculations with a CAS(10,8)/6-31G zero point energy correction for the HPA-$T_1(^3n\pi^*)$, HPA-$T_2(^3\pi\pi^*)$, HPA-$S_1(^1n\pi^*)$, HPA-$T_3(^3n\pi^*)$, HPA-$S_2(^1n\pi^*)$, HPA-$S_3(^1\pi\pi^*)$ ← HPA-S_0 transitions were similar to those found experimentally or from similar calculations for other related aromatic carbonyl systems and the energy gap between the ππ* and nπ* triplet states is small and similar to that observed for PhCHO.[29,30] The HPA-$T_2(^3\pi\pi^*)$ (72.9 kcal/mol) is located between the HPA-$T_1(^3n\pi^*)$ (71.5 kcal/mol) and HPA-$S_1(^1n\pi^*)$ (75.0 kcal/mol) in energy. These results are in agreement with the energy level ordering for a number of aromatic ketones determined from the phosphorescence excitation method including the closely related *p*-hydroxyacetophenone molecule.[21d,e] From comparison to closely related experimental and computational results,[21,25−30] our present computations give a reasonable estimate for the relative energies of the low-lying electronic states of *p*-hydroxyphenacyl acetate (HPA). The adiabatic transition energies are also consistent with relatively little differences in the electronic absorption spectrum and the very similar ultrafast photophysics (up to several ps) observed for HPA in both neat acetonitrile and mixed water/acetonitrile solvents.[15,16]

Our results indicate that it is difficult for either α or *β* bond cleavage reactions to occur from the S_1 excited state. In addition the S_1, T_1, and T_2 states are close in energy and the three $S_1(^1n\pi^*)$, $T_1(^3n\pi^*)$, and $T_2(^3\pi\pi^*)$ surfaces intersect at the same region (e.g. the HPA-T_1/T_2 and HPA-S_1/T_2 intersections occur in the same region). These preceding results suggest that intersystem crossing could be expected to be very fast and quickly depopulate the S_1 state to the nearby triplet states. This is consistent with and in good agreement with ultrafast spectroscopy experiments that show that the S_1 state ISC occurs within about 1−2 ps to form a triplet state for HPA and related *p*HP compounds.[15,16,39] The ultrafast ISC from the S_1 state to the nearby triplet state appears to be very similar for HPA and related *p*HP compounds in both neat acetonitrile and mixed water/acetonitrile solvents.[15,16,39]

Our computational results suggest that C8−C9 (or α) bond cleavage in the T_1 state has little dependence on the leaving group with barriers to scission of 15.9, 14.9, and 16.6 kcal/mol for HPA, HPDP, and HPPP, respectively, from the B3LYP/6-31G* level of theory with a zero point correction. On the other

hand, the C9−O10 (or β) bond cleavage in the T_1 state has a more noticeable dependence on the leaving group with barriers to scission of 17.4, 12.2, and 7.1 kcal/mol for HPA, HPDP and HPPP, respectively, from the B3LYP/6-31G* level of theory with a zero point correction. We also note that both the α C8−C9 and β C9−O10 bond cleavage reactions take place with fairly high barriers and compete with one another. This is not consistent with the photodeprotection reaction of HPA, HPDP, and HPPP in the aqueous and largely water containing solvents where the C9−O10 (or β) bond cleavage reactions are very fast and predominate to release the leaving group accompanied by a solvolytic rearrangement reaction to form the HPAA final product.[12,13,15,16] It is interesting to note that the trend of the leaving group dependence on the C9−O10 (or β) bond cleavage of 17.4, 12.2, and 7.1 kcal/mol for HPA, HPDP, and HPPP, respectively, predicted from the B3LYP/6-31G* level of theory with a zero point correction roughly follows the experimental observation of noticeably faster release of diphenyl phosphate from HPPP (time constant of about 150 ps) compared to diethyl phosphate from HPDP (time constant of about 350 ps).[16] This may be fortuitous or possibly reflect a leaving group dependence on the strength of the C9−O10 bond for the triplet state of *p*HP phototrigger molecules.

Our SCRF/PCM//B3LYP/6-31G* calculations suggest that C9−O10 (or β) bond cleavage in the nπ* triplet state is sensitive to the polarity of solvent while the barrier of the nπ* triplet state C8−C9 (or α) bond fission remains unchanged in gas phase and aqueous media (as well as in both polar and nonpolar solvents). These results imply that the α bond fission appears to be a homolytic dissociation that generates radical products in both the gas phase and aqueous media while the β bond cleavage exhibits some characteristics of a heterolysis mechanism in polar solvents. Similarly, studies by both Givens and co-workers and Falvey and co-workers suggested that the absence of decarboxylation (the β bond cleavage) products in polar solvents originated from a heterolysis dissociation leading to the conjugate base of the leaving group.[39] In our PCM calculations, water and acetonitrile cause the same influence upon the nπ* triplet state β bond cleavage (the barriers are lowered to be about 5.6 kcal/mol) in comparison with reaction in the gas phase. It should be noted the solvent effect does not appear to give a full explanation for experimental observations[15,16,39] in which the quantum yields of the deprotection (β bond cleavage) strongly depend on the water concentration. This suggests that water probably plays the role of a "reactant" rather than just being a solvent in the deprotection (β bond cleavage) process. It would be rewarding to investigate excited state calculations that take into account hydrogen bonding of water molecules explicitly to the HPA and related *p*HP phototrigger triplet states to examine how the strong water hydrogen bonding of the solvent shell probably triggers and participates in a very fast and efficient deprotection reaction for this interesting class of compounds. We plan to attempt these types of excited state reaction calculations in the future in order to better understand the details of the role of water in the deprotection reaction(s) of *p*HP phototrigger compounds.

Conclusion

The adiabatic electronic transition energies for the HPA-T_1(^{3}nπ*), HPA-T_2($^3\pi\pi$*), HPA-S_1(^{1}nπ*), HPA-T_3(^{3}nπ*), HPA-S_2(^{1}nπ*), HPA-S_3($^1\pi\pi$*) ← HPA-S_0 transitions from CAS(14,11)/6-31G* calculations with a CAS(10,8)/6-31G zero point energy correction were found to be similar to and in agreement with those found experimentally for closely related aromatic ketones such as *p*-hydroxyacetophenone[21d,e] as well as results from similar calculations for other related aromatic carbonyl systems. The calculated energy gap between the $\pi\pi$* and nπ* triplet states was found to be small and similar to that observed experimentally for PhCHO.[29,30] The HPA-T_2($^3\pi\pi$*) calculated transition was found to be between the HPA-T_1(^{3}nπ*) and HPA-S_1(^{1}nπ*) transitions in energy, in agreement with the energy level ordering derived from the phosphorescence excitation method for a range of aromatic ketones including the closely related *p*-hydroxyacetophenone molecule.[21d,e] The present calculations found that it is fairly difficult for either the α or β bond cleavage reactions to take place from the S_1 excited state and the S_1, T_1, and T_2 states are close in energy with the three S_1(^{1}nπ*), T_1(^{3}nπ*), and T_2($^3\pi\pi$*) surfaces intersecting at the same region. These results suggest that intersystem crossing can be very fast so that the S_1 state molecules quickly convert to the nearby triplet states, and this is consistent with results from ultrafast spectroscopy experiments that observe that the S_1 state ISC occurs within about 1−2 ps to produce a triplet state for HPA and related *p*HP compounds in both neat acetonitrile and mixed water/acetonitrile solvents.[15,16,39] Our calculations found that both the C8−C9 (or α) and C9−O10 (or β) bond cleavage reactions have fairly high barriers and compete with one another in the T_1 state. The mechanism of C9−O10 (or β) rather than C8−C9 (or α) bond cleavage in the nπ* triplet state is sensitive to the polarity of solvent. The solvent effects do not appear to fully explain the observation that the quantum yields of the deprotection (β bond cleavage) strongly depend on the water concentration. Comparison of our present computational results with experimental results for HPA and related *p*HP compounds suggests that water molecules probably have an important role in inducing a very fast and efficient deprotection to release the leaving group from the triplet state. In summary, our preliminary theoretical study for the excited states of the HPA phototrigger compound gave results consistent with the electronic spectroscopy and initial photophysics observed experimentally but is not entirely consistent with the very fast and efficient deprotection reaction from the triplet state observed experimentally.

Acknowledgment. This research was supported by a grant from the Research Grants Council of Hong Kong (HKU/7108/02P) to D.L.P. W.M.K. thanks the University of Hong Kong for the award of a Research Assistant Professorship.

Supporting Information Available: Cartesian coordinates, total energies, and vibrational zero-point energies for the stationary structures on the potential energy surfaces of the C8−O9 and C9−O10 fission for *p*-hydroxyphenacyl acetate (HPA). Cartesian coordinates, total energies, and vibrational zero-point energies for the stationary structures on the potential energy surfaces of the C8−O9 and C9−O10 fission for *p*-hydroxyphenacyl diethyl phosphate (HPDP) and diphenyl phosphate (HPPP). Cartesian coordinates, total energies, and vibrational zero-point energies for the stationary structures on the potential energy surfaces for the α and β bond fissions with consideration of solvent effects for *p*-hydroxyphenacyl acetate (HPA). This material is available free of charge via the Internet at http://pubs.acs.org.

References and Notes

(1) Givens, R. S.; Kueper, L. W. *Chem. Rev.* **1993**, *93*, 55−66 and references therein.

(2) Givens, R. S.; Athey, P. S.; Matuszewski, B.; Kueper, L. W., III; Xue, J. Y.; Fister, T. *J. Am. Chem. Soc.* **1993**, *115*, 6001−6012 and references therein.

(3) (a) Givens, R. S.; Athey, P. S.; Kueper, L. W., III; Matuszewski, B.; Xue, J.-Y. *J. Am. Chem. Soc.* **1992**, *114*, 8708−8710. (b) Gee, K. R.; Kueper, L. W., III; Barnes, J.; Dudley, G.; Givens, R. S. *J. Org. Chem.* **1996**, *61*, 1228−1233.

(4) (a) Il'ichev, Y. V.; Schworer, M. A.; Wirz, J. *J. Am. Chem. Soc.* **2004**, *126*, 4581−4595. (b) Rajesh, C. S.; Givens, R. S.; Wirz, J. *J. Am. Chem. Soc.* **2000**, *122*, 611−618. (c) Hangarter, M.-A.; Hörmann, A.; Kamdzhilov, Y.; Wirz, J. *Photochem. Photobiol. Sci.* **2003**, *2*, 524−535.

(5) Rock, R. S.; Chan, S. I. *J. Am. Chem. Soc.* **1998**, *120*, 10766−10767.

(6) Namiki, S.; Arai, T.; Rujimori, K. *J. Am. Chem. Soc.* **1997**, *119*, 3840−3841.

(7) (a) Lee, K.; Falvey, D. E. *J. Am. Chem. Soc.* **2000**, *122*, 9361−9366. (b) Banerjee, A.; Lee, K.; Yu, Q.; Fan, A. G.; Falvey, D. E. *Tetrahedron Lett.* **1998**, *39*, 4635−4638. (c) Banerjee, A.; Falvey, D. E. *J. Org. Chem.* **1997**, *62*, 6245−6251.

(8) Zou, K.; Miller, W. T.; Givens, R. S.; Bayley, H. *Angew. Chem., Int. Ed.* **2001**, *40*, 3049−3051.

(9) (a) Givens, R. S.; Weber, J. F. W.; Conrad, P. G., II; Orosz, G.; Donahue, S. L.; Thayer, S. A. *J. Am. Chem. Soc.* **2000**, *122*, 2687−2697 and references therein. (b) Conrad, P. G., II; Givens, R. S.; Weber, J. F. W.; Kandler, K. *Org. Lett.* **2000**, *2*, 1545−1547.

(10) (a) Givens, R. S.; Park, C.-H. *Tetrahedron Lett.* **1996**, *37*, 6259−6262. (b) Park, C.-H.; Givens, R. S. *J. Am. Chem. Soc.* **1997**, *119*, 2453−2463. (c) Givens, R. S.; Jung, A.; Park, C.-H.; Weber, J.; Bartlett, W. *J. Am. Chem. Soc.* **1997**, *119*, 8369−8370.

(11) Specht, A.; Loudwig, S.; Peng, L.; Goeldner, M. *Tetrahedron Lett.* **2002**, 6, 8947−8950.

(12) Conrad, P. G., II; Givens, R. S.; Hellrung, B.; Rajesh, C. S.; Ramseier, M.; Wirz, J. *J. Am. Chem. Soc.* **2000**, *122*, 9346−9347.

(13) Zhang, K.; Corrie, J. E. T.; Munasinghe, V. R. N.; Wan, P. *J. Am. Chem. Soc.* **1999**, *121*, 5625−5632.

(14) Brousmiche, D. W.; Wan, P. *J. Photochem. Photobiol., A* **2000**, *130*, 113−118.

(15) Ma, C.; Kwok, W. M.; Chan, W. S.; Zuo, P.; Kan J. T. W.; Toy, P. H.; Phillips, D. L. *J. Am. Chem. Soc.* **2005**, *127*, 1463−1427.

(16) Ma, C.; Kwok, W. M.; Chan, W. S.; Du, Y.; Kan J. T. W.; Toy, P. H.; Phillips, D. L. *J. Am. Chem. Soc.* **2006**, *128*, 2558−2570.

(17) Frisch, M. J.; Trucks, G. W.; Schlegel, H. B.; Scuseria, G. E.; Robb, M. A.; Cheeseman, J. R.; Montgomery, J. A.; Vreven, T., Jr.; Kudin, K. N.; Burant, J. C.; Millam, J. M.; Iyengar, S. S.; Tomasi, J.; Barone, V.; Mennucci, B.; Cossi, M.; Scalmani, G.; Rega, N.; Petersson, G. A.; Nakatsuji, H.; Hada, M.; Ehara, M.; Toyota, K.; Fukuda, R.; Hasegawa, J.; Ishida, M.; Nakajima, T.; Honda, Y.; Kitao, O.; Nakai, H.; Klene, M.; Li, X.; Knox, J. E.; Hratchian, H. P.; Cross, J. B.; Adamo, C.; Jaramillo, J.; Gomperts, R.; Stratmann, R. E.; Yazyev, O.; Austin, A. J.; Cammi, R.; Pomelli, C.; Ochterski, J. W.; Ayala, P. Y.; Morokuma, K.; Voth, G. A.; Salvador, P.; Dannenberg, J. J.; Zakrzewski, V. G.; Dapprich, S.; Daniels, A. D.; Strain, M. C.; Farkas, O.; Malick, D. K.; Rabuck, A. D.; Raghavachari, K.; Foresman, J. B.; Ortiz, J. V.; Cui, Q.; Baboul, A. G.; Clifford, S.; Cioslowski, J.; Stefanov, B. B.; Liu, G.; Liashenko, A.; Piskorz, P.; Komaromi, I.; Martin, R. L. Fox, D. J.; Keith, T.; Al-Laham, M. A.; Peng, C. Y.; Nanayakkara, A.; Challacombe, M.; Gill, P. M. W.; Johnson, B.; Chen, W.; Wong, M. W.; Gonzalez, C.; Pople, J. A. *Gaussian 03*, revision C.02; Gaussian, Inc.: Wallingford, CT, 2004.

(18) (a) Yang, N. C.; Dusenbery, R. *J. Am. Chem. Soc.* **1968**, *90*, 5899−5900. (b) Yang, N. C.; McClure, D. S.; Murov, S. L.; Houser, J. J.; Dusenbery, R. *J. Am. Chem. Soc.* **1967**, *89*, 5466−5468. (c) Long, M. E.; Lim, E. C. *Chem. Phys. Lett.* **1973**, *20*, 413−418. (d) Rauh, R. D.; Leermakers, P. A. *J. Am. Chem. Soc.* **1968**, *90*, 2246−2249. (e) Van Bergen, T. J.; Kellogg, R. M. *J. Am. Chem. Soc.* **1972**, *94*, 8451−8471.

(19) (a) Wagner, P. J. *Acc. Chem. Res.* **1971**, *4*, 168−177. (b) Wagner, P. J. *J. Am. Chem. Soc.* **1967**, *89*, 5898−5901. (c) Wagner, P. J.; Kemppainen, A. E. *J. Am. Chem. Soc.* **1968**, *90*, 5898−5899. (d) Wagner, P. J.; Truman, R. J.; Scaiano, J. C. *J. Am. Chem. Soc.* **1985**, *107*, 7093−7097.

(20) (a) Lamola, A. A.. *J. Am. Chem. Soc.* **1970**, *92*, 5045−5048. (b) Hochstrasser, R. M.; Marzzacco, C. *J. Chem. Phys.* **1968**, *49*, 971−984. (c) Li, Y. H.; Lim, E. C. *Chem. Phys. Lett.* **1970**, *7*, 15−18.

(21) (a) Beckett, A,; Porter, G. *Trans. Faraday Soc.* **1963**, *59*, 2051−2057. (b) Porter, G.; Suppan, P. *Trans. Faraday Soc.* **1965**, *61*, 1664−673. (c) Yang, N. C. *Reactivity of the Photoexcited Organic Molecule*; Interscience: London, 1967; p 150. (d) Kearns, D. R.; Case, W. A. *J. Am. Chem. Soc.* **1966**, *88*, 5087. (e) Case, W. A.; Kearns, D. R. *J. Phys. Chem.* **1970**, *52*, 2175−2191.

(22) Arnold, D. R. *Adv. Photochem.* **1968**, *6*, 301−426.

(23) Leigh, W. J.; Arnold, D. R.; Humphreys, R. W. R.; Wong, P. C. *Can. J. Chem.* **1980**, *58*, 2537−2549.

(24) Loutfy, R. O.; Loutfy, R. P. *Tetrahedron* **1973**, *29*, 2251−2252.

(25) Fang, W. H.; Phillips, D. L. *ChemPhysChem* **2002**, *3*, 889−892.

(26) Fang, W. H.; Phillips, D. L. J. *Theor. Comput. Chem.* **2003**, *2*, 23−31.

(27) He, H. Y.; Fang, W. H.; Phillips, D. L. *J. Phys. Chem. A* **2004**, *108*, 5386-5392.

(28) Chen, X. B.; Fang, W. H. *J. Am. Chem. Soc.* **2004**, *126*, 8976−8970.

(29) Ohmori, N.; Suzuki, T.; Ito, M. *J. Phys. Chem.* **1988**, *92*, 1086−1093.

(30) Ridley, J. E.; Zerner, M. C. *J. Mol. Spectrosc.* **1979**, *76*, 71−85.

(31) Silva, C. R.; Reilly, J. P. *J. Phys. Chem.* **1996**, *100*, 17111−17123 and references therein.

(32) Warren, J. A.; Bernstern, E. R. *J. Chem. Phys.* **1986**, *85*, 2365−2367.

(33) King, R. A.; Allen, W. D.; Schaefer, H. F., III. *J. Chem. Phys.* **2000**, *112*, 5585−5592 and references therein.

(34) Diau, E. W.-G.; Kotting, C.; Zewail, A. H. *ChemPhysChem* **2001**, *2*, 273−293; *ChemPhysChem* **2001**, *2*, 294−309 and references therein.

(35) Fang, W. H.; Liu, R. Z. *J. Chem. Phys.* **2001**, *115*, 10431−10437.

(36) Chen, X. B.; Fang, W. H. *Chem. Phys. Lett.* **2002**, *361*, 473−482.

(37) Chen, X. B.; Fang, W. H.; Fang, D. C. *J. Am. Chem. Soc.* **2003**, *125*, 9689−9698.

(38) Wagner, P. J.; Lindstrom, M. J. *J. Am. Chem. Soc.* **1987**, *109*, 3062−3067.

(39) Givens, R. S.; Lee, J., III. *J. Photosci.* **2003**, *10*, 37−48.